DOI: https://doi.org/10.67656/njmse.2020.7s236ddz

Olasupo et al. Nigerian Journal of Materials Science and Engineering. Vol. 10(2):68 - 80 (2020)

Green Synthesis and Characterisation of Magnetite Nanoparticles Using Factorial Design of Experiment

[1,4,*]**Olasupo** Olayode Adesola, [1,3]**Abdulkareem** Ambali Saka [1,3]**Kovo** Abdulsalami. Sani and [1,2]**Abubakre** Oladiran Kamardeen.

[1]Nanotechnology Research Group, Africa Centre of Excellence for Mycotoxin and Food Safety, Federal University of Technology, Minna, NIGERIA

[2]Materials and Metallurgical Engineering Department, Federal University of Technology, Minna, NIGERIA

[3]Chemical Engineering Department, Federal University of Technology, Minna, NIGERIA

[4]Engineering Infrastructure Department, National Agency for Science and Engineering Infrastructure, Idu Industrial Area, PMB 391, Garki, Abuja, NIGERIA

*Corresponding Author: solayode@gmail.com.

Abstract

Magnetite nanoparticles have been produced by green synthesis method. Aqueous extract of *Mangifera indica* leaves was used as reducing agent for co-precipitation of magnetite from iron (II) and iron (III) salts in 1:2 molar ratio. Optimisation of the process was carried out using 2^3 factorial design of experiments taking into consideration stirring time of reaction medium, temperature and volume of extracts with hdrodynamic particle size as response. A 2^2 factorial design was afterwards conducted with temperature of reaction medium and volumetric ratio of plant extracts to iron precursor as factors and hydrodynamic particle size as response. Characterisation of the nanoparticles was done using UV-visible spectrometer, Dynamic Light Scattering (DLS) method for hydrodynamic particle size measurement, X-ray diffraction (XRD) and High Resolution Transmission Electron Microscopy (HRTEM). Results obtained reveals that the best parameter for the synthesis of magnetite nanoparticles is a volume of precursor to plant extract ratio of 1:15 at a temperature of 70°C. Measurement of particle size of the magnetite nanoparticles using DLS method gave an average hydrodynamic particle size of 143.9 nm; the particles size measurement using Scherer's equation from the XRD spectra gave 52.04 nm, while the High Resolution Transmission Electron Microscopy result indicated that the nanoparticles are spherical in nature, with a mean particle size of approximately 9 nm. It can be inferred from the analyses that, ratio of iron precursors to plant extract, temperature, and stirring time, played important roles in size of particles.

Keywords: Optimisation, Magnetite, Nanoparticles, Factorial Design.

1.0 INTRODUCTION

Magnetite (Fe_3O_4) is a naturally occurring iron oxide which has a distinguishing characteristic of being the most magnetic of all the minerals on earth (Pranita and Preeti, 2015). Magnetite nanoparticles having dimensions between 1 and 100 nm find applications in the field of drug delivery (Vangijzegem, *et al*., 2019; Wallyn, *et al*., 2019; Price, *et al*., 2018; Mody, *et al.,* 2014), antibacterial activities (Sathishkumar, *et al*., 2018; Kanagasubbulakshmi and Kadirvelu 2017), catalytic activities (Prasad *et al*., 2016), adsorption of heavy meals ions and dyes from wastewater (Bibi *et al*., 2019; Ramesh, *et al*., 2018; Ruíz-Baltazara *et al*., 2018), as sensitive contrast agents for magnetic resonance imaging (Cormode *et al*., 2009), multifunctional magnetic particles enabling the diagnosis and therapy at the same time (Kudri *et al*., 2017), enhancement of sensitivity and stability of sensors and biosensors for the detection of several analytes in clinical, food and environmental applications (Rocha-Santos, 2014).

Magnetite nanoparticles have been produced by mechanical attrition, where the mineral ore is physically broken down from micrometer to nanometer dimension, using high energy mills. The process is expensive because of high energy requirement (Prasad 2014; Saif *et al*., 2016). Synthesis of magnetite nanoparticles by chemical co-precipitation method has been extensively investigated based on the mechanism of magnetite formation involving Fe^{2+} and Fe^{3+} ions, in molar ratio of 1:2, reacting in alkaline conditions. The overall reaction is as presented in Equation 1, adapted from Mascolo *et al*. (2013).

$$2FeCl_3+FeCl_2+8\boldsymbol{X}OH = Fe_3O_4(s)+4H_2O+8\boldsymbol{X}Cl \qquad (1)$$

Where $\boldsymbol{X}$= Na+, K+ or $(C_2H_5)_4N^+$

Chemical synthesis route, though simpler in approach contribute to more chemical usage in production processes and hence more environmental pollution. The biosynthesis approach of magnetite production (microbes and plant mediated synthesis) involves the use of microorganisms or plant extracts as reducing and capping agents for the production of magnetite nanoparticles. However, Al-Kalifawi (2015) noted that the microbes employed during production processes can be pathogenic and risky to handle. The biosynthesis approach is cost effective,

Copyright Reserved © NJMSE, 2020

environmentally friendly and promising in its application in medicine and wastewater treatment (Latha and Gwori, 2014) with the ability to control the size and shape of nanoparticles and its properties during synthesis (Prasad, 2014). Meanwhile, plant extracts act as low cost reducing and stabilizing agents in synthesis of nanoparticles. Polyphenol capping around nanoparticles produced by green synthesis enables its use in water purification and also in remediation of ground water (Herlekar *et al*., 2014). The fact that magnetite nanoparticles production using plant extract is carried out at room temperature or by hydrothermal synthesis by mixing plant extracts and metal salts solution in a fixed ratio makes this route economical and hence attractive to researchers (Herlekar *et al*., 2014). The plants parts are readily available in nature and are therefore more preferred biological resources than microbes (Herlekar, *et al*., 2014).

Recent works on green synthesis of magnetite nanoparticles have indicated the mechanisms behind the reduction and capping of the nanoparticles. It follows the chemical reduction method with the substitution of the base with the secondary metabolites from the plant extracts containing the hydroxyl groups. Some of these secondary metabolites are phenolic compounds; polyphenols, tanins and alkaloids. The plant extracts act as reducing and capping agents in the formation of magnetite. The appearance of black colour usually indicates the formation of magnetite. This was confirmed by several authors (Awwad and Salem, 2012; Herlekar *et al*., 2014, Latha and Gwori, 2014). Awwad and Salem (2012) proposed that protein chains of carob leaves extract acted as capping and stabilizing agent. Meanwhile, Karkuzhali and Yogamoorthi, 2015, proposed that terpenoid, steroids, saponin, flavinoid and triterpenoid together or individually might have reduced ferric chloride into iron oxide.

Literature survey revealed that more research needs to be done on the optimisation of the green synthesis of magnetite nanoparticles. There is therefore the need to do more studies in this direction and also to upscale the synthesis routes for industrial production and applications. The full factorial design of experiment is therefore used in this study to optimise the synthesis of magnetite nanoparticles.

2.0 MATERIALS AND METHOD

2.1 Materials

The materials used for the research are plant parts which include orange (*Citrus sinensis*) peel, pawpaw (*Carica papaya*) leaves, mango (*Mangifera indica*) leaves and almond (*Terminalia cattapa*) leaves. All the plant parts were collected from the Bosso Campus of Federal University of Technology, Minna. Analytical reagents; $FeCl_2.4H_2O$ and $FeCl_3$ were purchased from SISCO Research Laboratories Pvt. Ltd. Mumbai, India and Polyethylene Glycol (PEG 2000) from Merck KGaA, Germany. All chemicals were used without further purification. De-ionised water was used for all synthesis procedures.

2.2 Methods

2.2.1 Phytochemical screening of plant parts

The plant parts; (*Citrus sinensis*) peel, pawpaw (*Carica papaya*) leaves, mango (*Mangifera indica*) leaves and almond (*Terminalia cattapa*) leaves were dried naturally at room temperature on a laboratory bench for 28 days. They were thereafter crushed and ground into fine powder. The ground samples were passed through 150 μm sieve and the oversized rejected. The sieved samples were thereafter kept in laboratory sterile sample bottles for further analysis. A known weight, 1.0 g each of pulverized mango leaves, almond leaves, pawpaw leaves and orange peels were measured and kept in laboratory sterile bottles and used for phytochemical screening. The samples were thereafter tested for qualitative and quantitative analyses of tannin, flavonoid and total phenol (Association of Official Analytical Chemists, 1984).

2.2.2 Aqueous extraction of phytochemicals from *Mangifera indica* leaves

Aqueous extract of *Mangifera indica* was chosen for the further analysis due to its high total phenol content. A known weight (10 g) of *Mangifera indica* powdered leaf sample was added to 200 mL of deionised water in a 250 mL laboratory beaker. The mixture was heated until boiling at 100 ^{o}C for 5 min. It was then allowed to cool to room temperature and filtered. The filtrate was kept in a refrigerator.

2.2.3 Synthesis of magnetite nanoparticles

Co-precipitation method (Mascolo *et al*., 2013) was used to produce the magnetite nanoparticles. $FeCl_3$ (anhydrous) and $FeCl_2.4H_2O$ were used as metal ions precursor, while aqueous extract of *Mangifera indica* leaves due to its high percentage of phenols was used as reducing agent. The precursors were prepared in Fe^{3+}:Fe^{2+} ratio of 2:1 to obtain the right proportion of iron ions in the stoichiometric chemical formula of magnetite as presented in Equation 2.

$$2Fe^{3+}+Fe^{2+}+8OH^{-} \quad Fe_3O_4+4H_2O \qquad (2)$$

The OH^{-} came from the phenolic groups in the aqueous plant extract.

A known volume of 50 mL, 0.2 M $FeCl_3$ was prepared by dissolving 1.622 g of the (anhydrous)

Copyright Reserved © NJMSE, 2020

salt in deionised water and making it up to 50 mL mark in a measuring cylinder. Another 50 mL of 0.1 M $FeCl_2.4H_2O$ was prepared by dissolving 0.984 g of the salt in 40 mL of deionised water, and then making the solution up to 50 mL mark in a measuring cylinder. The Fe^{3+} and Fe^{2+} salts were then added together to obtain 100 mL of the precursor. The mixture was stirred until the salts were totally dissolved. The mixture was used immediately for the preparation of various ratios of magnetite nanoparticles formulation to prevent oxidation of the Fe^{2+} to Fe^{3+}. Mango leaves extracts were added to a fixed volume of the precursor in the following precursor:extract ratios of 1:1, 1:5, 1:10, 1:15 and 1:20. The colour of the reaction mixture changed instantly from golden yellow for the iron precursors and brown for the aqueous mango leaves extract to black. This signified the formation of magnetite nanoparticles.

Samples were taken from each of the magnetite nanoparticles suspensions and diluted in ratio sample:deionised water of 1:100 for UV-Visible spectrum analysis. The absorbance peaks for the magnetite nanoparticles were found to be optimum for the production of magnetite for the values of precursor:extract ratio of 1:10 and 1:15. These values were therefore optimized at lower temperature of 30°C and upper temperature of 70°C for the production of magnetite nanoparticles using the 2^3 Full Factorial Design of Experiment. The three reaction parameters: volumetric ratio of plant extract to Fe^{2+}+Fe^{3+} precursor, temperature and stirring time with their upper and lower levels are presented in Table 1. The detailed factorial design matrix for the magnetite nanoparticles production is presented in Table 2.

Further experiments were carried out in optimising the magnetite nanoparticles production without stirring the reaction medium. A 2^2 full factorial design of experiment was conducted**.** The two reaction parameters: volumetric ratio of plant extract to Fe^{2+}+Fe^{3+} precursor and temperature with their upper and lower levels are presented in Table 3, while the detailed factorial design matrix for the magnetite nanoparticles production is presented in Table 4.

Table 1: Levels and Factors Considered in 2^3 Optimisation of Magnetite Nanoparticles Production

	Volumetric Ratio of Plant Extract to Fe^{2+}+Fe^{3+} Precursor	Temperature (°C)	Stirring Time (min)
Upper (+) Level	15:1	70	60
Lower (-) Level	10:1	30	30

Table 2: 2^3 Factorial Design of Experiment for Optimisation of Magnetite Nanoparticles Production

Run Order	Volumetric Ratio of Plant Extract to Fe^{2+}+Fe^{3+} Precursor	Temperature of Reaction (°C)	Stirring Time (min)	Response, UV-Visible Wavelength	Response, Hydrodynamic Particle Size, (nm)
1	10:1	30	30		
2	15:1	70	30		
3	15:1	30	60		
4	10:1	30	60		
5	15:1	70	60		
6	15:1	30	30		
7	10:1	70	60		
8	10:1	70	30		

Table 3: Levels and Factors Considered in 2^2 Optimisation of Magnetite Nanoparticles Production

	Volumetric Ratio of Plant Extract to Fe^{2+}+Fe^{3+} Precursor	Temperature of Reaction (°C)
Upper (+) Level	15:1	70
Lower (-) Level	10:1	30

Copyright Reserved © NJMSE, 2020

Table 4: 2^2 Factorial Design of Experiment for Optimisation of Magnetite Nanoparticles Production

Run Order	Volumetric Ratio of Plant Extract to Fe^{2+}+Fe^{3+} Precursor	Temperature of Reaction (°C)	Response, Hydrodynamic Particle Size (d,nm)
1	10:1	30	
2	10:1	70	
3	15:1	30	
4	15:1	70	

2.3 Characterisation of Magnetite Nanoparticles.

2.3.1 UV-visible spectrophotometry measurements

The UV-visible absorption spectrophotometry was done using the UV-spectrometer, UV-1800, manufactured by SHMADZU, Japan. Liquid samples (2 cm^3) were measured into the cuvette. The UV-spectrometer was then connected to the computer. Deionised water was used as blank for the readings. The deionised water sample was first scanned as the blank for the measurements before the samples were scanned.

2.3.2 X-Ray diffraction studies

A known weight (2.0 g) of magnetite nanoparticles sample was placed in a sample holder. The voltage and the current of the X-Ray machine were set for the X-Ray source and the computer software was activated for copper Kα wavelength (Cu Kα) of 1.5406 Å. The machine was calibrated using pure silicon standard sample. After calibration, the sample was loaded and diffraction patterns were recorded on the machine at room temperature within the range of 3 to 90° on the 2θ scale with a scanning speed of 0.05 °/s. At the end of the scan, the d-spacing for each peak was calculated from the 2θ values. The interplanar spacing for diffraction angle of each peak (d-spacing), calculated using Braggs law (Equation 3) was compared with the search and match routine of the d-spacing of known materials with the d-spacing of unknown materials.

$$n\lambda = 2d \sin\theta \qquad (3)$$

where λ = wavelength of X-Ray = 1.5406 Å, d = d-spacing in Å, θ = Diffraction angle in radians.

The unit cell parameters were calculated and indexed as *hkl*. The average crystallite size of the sample was calculated from the analysis of the peaks in the X-Ray diffraction pattern using Scherer's Equation as presented in Equation 4 (Monshi *et al*., 2012).

$$D = \frac{K\lambda}{\beta \cos\theta} \qquad (4)$$

where K= Scherer's constant = 0.9, λ = wavelength of X-Ray, β = Full Width at Half Maximum, θ = Diffraction angle in radians.

2.3.3 High resolution transmission electron microscopy

Transmission Electron Microscopy was done using TECNAI G2 F20 twin model Transmission Electron Microscope. 0.02 g of magnetite nanoparticles sample was suspended in 100 mL of methanol. The mixture was then ultrasonicated for proper dispersion of the sample. A few drops of the slurry were thereafter put onto the carbon grid using a micropipette. This was then dried under photo-light. After drying, the carbon grid was loaded onto slit sample holder and then mounted on the shaft of the Transmission Electron Microscope for analyses. Other experimental conditions are illumination angle of the machine, 15°, Electron High Tension of 200 kV, resolution of 0.24 nm, spot size of 3 nm, gun lens of 1 nm, objective aperture of 2 nm, condenser aperture of 3 nm, emission current of 54 µA and extraction voltage of 3950 V.

2.3.4 Hydrodynamic particle size analysis

Particle size analysis of the magnetite nanoparticles was done using the Nano-S zetasizer instrument. The hydrodynamic diameters of samples were determined using the Malvern Nanozetasizer, Nano-S equipment. 0.1 mL of the liquid sample was dispersed in 10 mL of de-ionised water at room temperature. This was done to avoid the effect of Brownian motion on the particles. The dispersed sample was then filtered directly into a polystyrene cuvette using a 0.22 µm filter attached to a syringe. The cuvette was thereafter placed inside the laser chamber of the machine for analysis. The sample was left in the chamber for 120 min to equilibrate before the reading was taken. Other operating conditions were temperature of 25°C and laser scattering angle of 173°. The magnetite nanoparticle sample was run five times and the average of the results was recorded.

2.3.5 Measurement of Magnetic Properties

The magnetic properties of the magnetite nanoparticles were measured using the vibrating sample magnetometer, model number C6325-06 manufactured by Microsense Corporation, Massachusetts, USA.

Copyright Reserved © NJMSE, 2020

3.0 RESULTS AND DISCUSSIONS

3.1 Phytochemical Screening of Plant Parts

Prior to the green synthesis of the magnetite nanoparticles, the plant parts procured for the synthesis were screened and the results obtained are presented in Table 5. This was done in an attempt to choose the best plant with the necessary phytochemicals for magnetite nanoparticles production. The results of the phytochemical analysis revealed the presence of tannin, flavonoid and phenol in varying quantities in all the plant extracts. The mechanism of reactions during the production of iron oxide nanoparticles using plant extracts has been difficult to establish (Veeramanikandan *et al*., 2017).

Meanwhile, the organic chemicals (phytochemicals); alkaloids, phenolic acid, flavonoid, tannins, terpenoids and carbohydrates, have been reported to act as reducing and capping agent for the synthesis of magnetite nanoparticles (Ramesh *et al*., 2108). Polyphenols have equally been reported to act as both reducing and capping agent resulting in stable, green nanoscale zerovalent iron particles (Saif, *et al*, 2016). Therefore, the higher concentration of total phenol and flavonoid in the mango leaves extract favoured its choice as reducing agent in the green synthesis of magnetite nanoparticles and was therefore used for the optimisation of the synthesis of magnetite nanoparticles.

Table 5: Phytochemical Screening of Plants

Plant Part	Total Phenol (mg/g)	Flavonoid (mg/g)	Tannin (mg/g)
Orange Peel	0.048	0.0183	0.87
Almond Tree Leaves	4.730	0.0462	1.20
Mango Leaves	5.348	0.0183	0.90
Pawpaw Leaves	1.107	0.0183	0.61

3.2 Effect of Volume of Metal Precursors to Volume of Extract on the Synthesis of Magnetite Nanoparticles

A preliminary study on the effect of the ratio of volume of metal precursor to the volume of extract on the formation of the magnetite nanoparticles was done before the optimisation process. This was required to determine the upper and lower levels to be used in the full factorial design of experiment. UV-visible spectrometer only was used for the characterisation of the samples at this stage. This was done to observe the formation of absorbance peaks and the Surface Plasmon Resonance (SPR) corresponding to the formation of magnetite nanoparticles after formation of the black coloured magnetite.

The results of the UV Visible spectrometry of the synthesised magnetite nanoparticles are presented in Figure 1 and Table 6. It was observed that the wavelength of the SPR absorption peaks decrease progressively from 263 nm in the sample produced with volume of iron precursor:volume of plant extract 1:1 (MNPM1) to 258 nm in sample produced with volume of iron precursor:volume of plant extract 1:10 (MNPM10) and then remains constant. The absorption peaks obtained for samples MNPM10 and samples produced with volume of iron precursor:volume of plant extract 1:15 (MNPM15) were distinct with formation of only one peak each; this gave an indication of synthesis of a single phase component. This peak also falls within the range of peak formations for synthesis of magnetite nanoparticles using plant extracts as observed by Pattannayak and Nayak (2013) which recorded the surface Plasmon resonance at 216 – 265 nm region. In the works of Awwad and Salem (2012), Surface Plasmon Resonance band of 233 nm was observed for synthesised magnetite nanoparticles from Fe^{2+}:Fe^{3+} (1:2) and fixed volume (5 mL) of aqueous carob leaf extract. Karkhuzali and Yogamoorthi (2015) observed the absorbance peak at 277 nm. Though, the sample produced volume of iron precursor:volume of plant extract 1:20 (MNPM20) gave an absorbance peak at 258 nm, there was appearance of noise in the UV spectrum at about 190 nm. This signifies some impurities in the synthesised magnetite nanoparticles. Therefore, the optimum ratio for the synthesis of magnetite nanoparticles at room temperature could be suggested between 1:10 and 1:15 of metal precursors:plant extract. These values were therefore picked for further investigations using a 2^3 factorial design to study the effect of volume of precursor:volume of plant extract, temperature and stirring time of the reaction mixture on the production of magnetite nanoparticles.

3.3 Optimisation of Magnetite Nanoparticles Synthesis

The influence of synthesis parameters (volume of plant extracts to precursor, temperature and stirring time) on particle size of the magnetite nanoparticles was investigated using 2^3 factorial. UV-visible spectrometry and hydrodynamic particle size analysis by dynamic light scattering method was used for characterisation of samples at this stage. The results for the UV-Visible spectrometry of the optimisation of the magnetite production in the study of the effect of volume of plant extract to precursors, stirring time and reaction temperature indicates that the shortest wavelength obtained was

Copyright Reserved © NJMSE, 2020

233 nm (Table 7) with the sample with volumetric ratio of plant extract to Fe^{2+}+Fe^{3+} precursor of 15:1 at temperature of 70 °C and stirring speed of 30 min. The sample equally had a distinct peak in the UV-spectrum (Figures 2 and 3). This wavelength was also observed by Awwad and Salem (2012) for the synthesis of black coloured magnetite nanoparticles synthesised from Fe^{3+} and Fe^{2+} ions in 2:1 molar ratio. A reduction in the wavelength as compared to the other reaction mixtures signifies a lower particle size material was synthesised. This sample equally gave a distinct peak in the UV- spectrum.

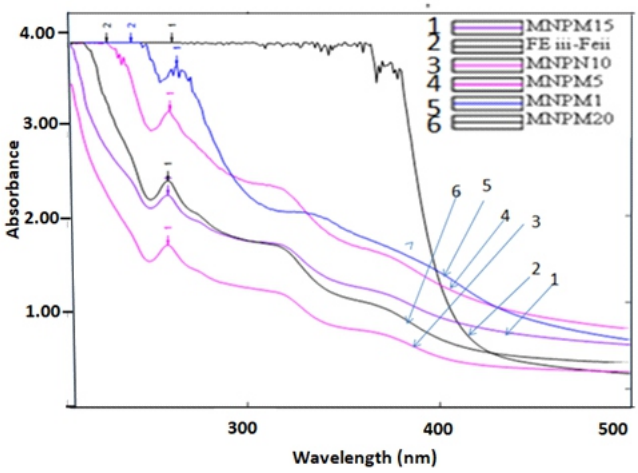


Figure 1: Effect of Volume of Plant Extract on the Production of Magnetite Nanoparticles.

Table 6: UV-Visible Spectrum of Magnetite Nanoparticles volume of extract to a fixed Volume of Iron Compounds

Sample Name	Volume of Precursor (mL)	Volume of Plant Extract (mL)	UV-Visible Wavelength (nm)
Fe III-FEII	1	0	Not Available
MNPM1	1	1	263
MNPM5	1	5	259
MNPM10	1	10	258
MNPM15	1	15	258
MNPM20	1	20	258

The particle sizes of the magnetite nanoparticles were obtained by Dynamic Light Scattering (DLS) Method and the results of the influence of synthesis parameters on the hydrodynamic particle size of the synthesised magnetite nanoparticles are presented in Table 7.

The sample codenamed MNPM10-30-30 refers to the sample prepared using volume of plant extract:iron precursor 10:1 at a temperature of 30°C

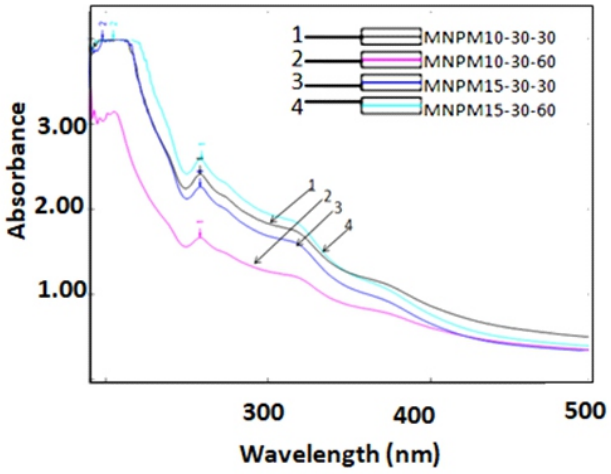


Figure 2: Effect of Volume of Extract and Stirring Time on Room Temperature Production of Magnetite nanoparticles

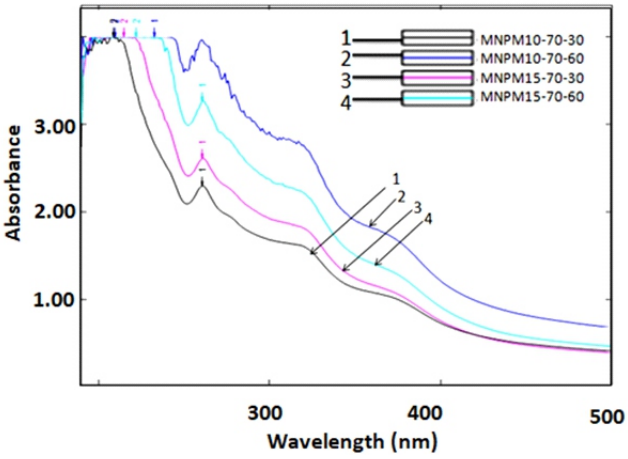


Figure 3: Effect of Volume of Extract and Stirring Time on Production of Magnetite nanoparticles at 70 °C

and stirring time of 30 min. Sample codenamed MNPM15-70-30 refers to the sample prepared using volume of plant extract:iron precursor 15:1 at a temperature of 70 °C and stirring time of 30 min. Sample codenamed MNPM15-30-60 refers to the sample prepared using volume of plant extract:iron precursor 15:1 at a temperature of 30°C and stirring time of 60 min. Sample codenamed MNPM10-30-60 refers to the sample prepared using volume of plant extract:iron precursor 10:1 at a temperature of 30 °C and stirring time of 60 min. Sample codenamed MNPM15-70-60 refers to the sample prepared using volume of plant extract:iron precursor 15:1 at a temperature of 70 °C and stirring time of 60 min. Sample codenamed MNPM15-30-30 refers to the sample prepared using volume of plant extract:iron precursor 15:1 at a temperature of 30 °C and stirring time of 30 min. sample codenamed MNPM10-70-60 refers to the sample prepared using

Copyright Reserved © NJMSE, 2020

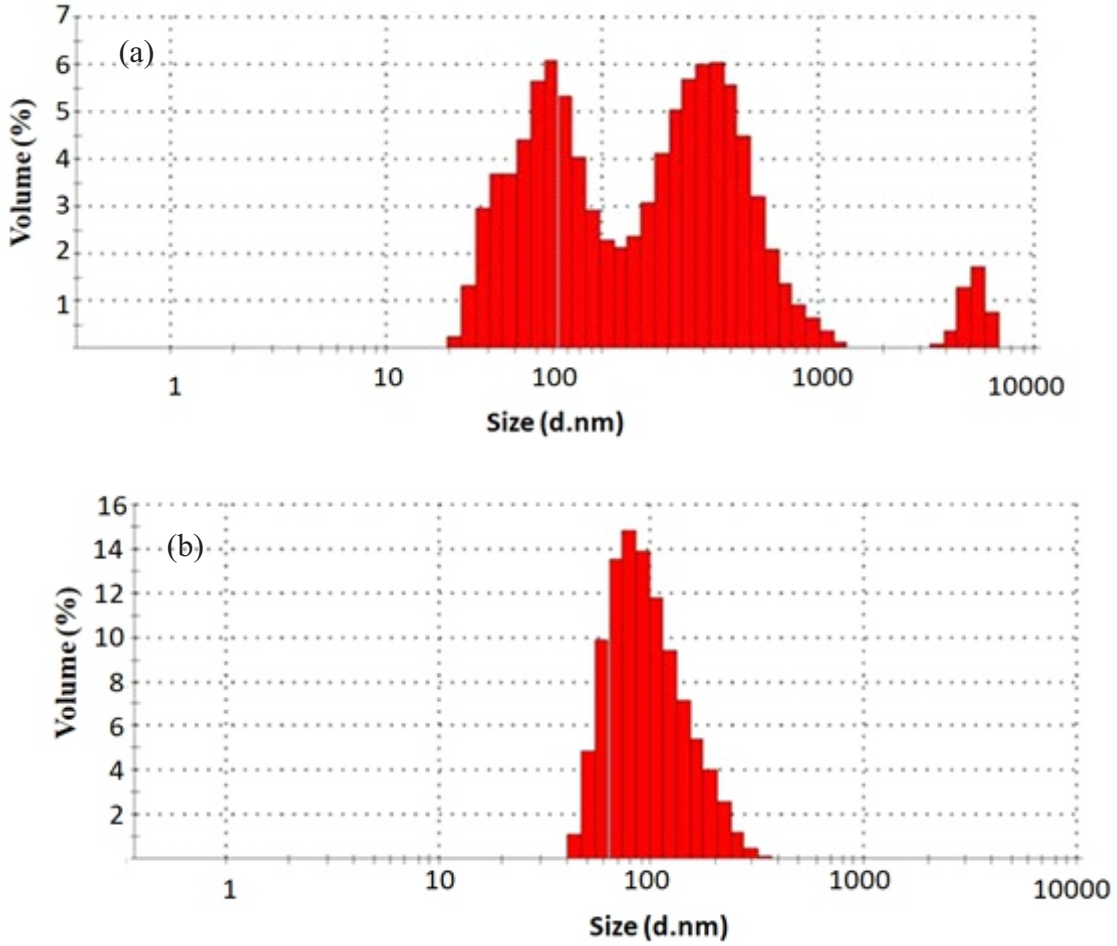


Figure 4: (a) Particle Size Distribution By Volume of Magnetite Nanoparticles Synthesised With volume of extract:volume of precursor 15:1 at 70 °C (a) in de-ionised water and (b) with 5 % v/v of PEG-2000 in deionised water determined by Dynamic Light Scattering method

PEG – 2000 (Figure 4(b)), there was proper dispersion of the nanoparticles resulting in a single range of particle size distribution in the nanosized range. PEG-2000 was therefore able to coat the surface of the nanoparticles and reduced magnetic attraction between them. The magnetite nanoparticles in Run order 4, stabilised with PEG-2000 was selected for further characterisation to determine using XRD and High Resolution Transmission Electron Microscopy respectively.

3.4 X-ray Diffraction Studies of Magnetite Nanoparticles

The XRD pattern of the magnetite nanoparticles synthesised with volume of extract:volume of precursor 15:1 at 70°C is presented in Figure 5 while the XRD parameters are presented in Table 10. Crystalline peaks were observed at 2-theta values of 21.34, 28.2, 35.43, 40.48, 43.67, 55.37, 58.08 and 68.13 corresponding to planes (111), (220), (311), (222), (400), (422), (511) and (620) respectively. Similar peaks were obtained by Lemes *et al* (2014); Ramesh *et al* (2018); and Priyadarshana *et al* (2015). The intense peak at (311) plane is commonly used for identification and calculation of crystallite size of magnetite (Lemes *et al.*, 2014). This peak from calculation using Scherer's Equation has a crystallite size of 31.28 nm (Table 9). The mean crystallite size of the particles when all the peaks were considered and calculated from Scherer's Equation was 52.04 nm. The intense reflection at (311) plane has also been reported to specify the growth direction of magnetite nanoparticles (Ramesh *et al.*, 2018).

The noise experienced on the X-ray diffraction pattern is due to the leaf extracts, which are non-crystalline materials and also constituted some impurities in the magnetite nanoparticles.

3.5 High Resolution Transmission Electron Microscopy

The morphology of the produced magnetite nanoparticles with volume of extract:volume of precursor 15:1 at 70°C was studied using the High resolution Transmission Electron Microscope. The transmission electron micrograph of the magnetite

Copyright Reserved © NJMSE, 2020

Table 7: Effect of Volume of Extract, Temperature and Stirring Time on the UV-Visible Spectrum and Particle size of Magnetite Nanoparticles Production

Run Order	Sample Name	Volumetric Ratio of Plant Extract to Fe^{2+}+Fe^{3+} Precursor	Temperature of Reaction (°C)	Stirring Time (min)	Response, UV-Wavelength, (nm)	Response, Hydrodynamic particle size, (d.nm)
1	MNPM10-30-30	10:1	30	30	258	836.2
2	MNPM15-70-30	15:1	70	30	233	470.1
3	MNPM15-30-60	15:1	30	60	259	1166
4	MNPM10-30-60	10:1	30	60	258	720.0
5	MNPM15-70-60	15:1	70	60	261	525.6
6	MNPM15-30-30	15:1	30	30	258	721.1
7	MNPM10-70-60	10:1	70	60	251	1051
8	MNPM10-70-30	10:1	70	30	261	505.1

volume of plant extract:iron precursor 10:1 at a temperature of 70°C and stirring time of 60 min. sample codenamed MNPM10-70-30 refers to the sample prepared using volume of plant extract:iron precursor 10:1 at a temperature of 70°C and stirring time of 30 min. The particle sizes of the synthesis carried out at 30°C are larger than those carried out at 70°C. This indicates that formation of small sized particles is favoured by higher temperature. It was also observed that particle size for the synthesis under the same condition of volume of extract and temperature are larger for higher time of stirring. This could be attributed to the strong magnetism exhibited by the particles which caused them to agglomerate and grow in size immediately after synthesis. Results as presented also indicate that the size of particles synthesised with these parameters are greater than 100 nm. Therefore the 2^2 factorial of experiment was conducted with the effect of volume of extracts and temperature without the stirring time. This allows the particle size to be measured by DLS immediately after synthesis. The result of the optimisation using 2^2 factorial design of experiment is presented in Table 8.

Table 8: Effect of Volume of Plant Extract and Temperature on the Particle size of Magnetite Nanoparticles

Run Order	Sample Name	Volumetric Ratio of Plant Extract to Fe^{2+}+Fe^{3+} Precursor	Temperature of Reaction (°C)	Hydrodynamic Particle Size (d.nm)
1	MNPM10-30	10:1	30	1317
2	MNPM10-70	10:1	70	446.2
3	MNPM 15-30	15:1	30	638.8
4	MNPM15-70	15:1	70	247.2

The average particle size measurements presented in Table 8 indicated that the sample in Run 4 which was synthesised using volumetric ratio of plant extract to iron precursor 15:1 and temperature of 70°C (MNPM15-70) has the lowest particle size of 247.2 nm. Addition of 5 % Polyethylene Glycol (PEG-2000) to the sample immediately after synthesis reduced the average particle size to 143.9 nm. Hence PEG-2000 has the capacity to further disperse the nanoparticles and prevent agglomeration due to magnetic attraction between them.

The particle size distribution of the magnetite nanoparticles, in percent volume, measured as hydrodynamic diameter (d.nm) is presented in Figure 4(a) and (b) respectively. Figure 4(a) presents the particle size distribution of the magnetite produced with volumetric ratio of plant extract to Fe^{2+} + Fe^{3+} precursor of 1:15 at a temperature of 70°C (Run 4), while Figure 4 (b) presents magnetite nanoparticles produced under the same condition but stabilised by addition of 5% v/v of PEG-2000.

The particle size distribution in Figure 4 (a) depicts three-modal distribution, indicating formation of three peaks in the size distribution. The first indicates the particles in the nanometer range *(i)*; the second indicates the particles between the nano sized range and micron range *(ii)*; the third were the particles which are purely in the micron sized range *(iii)*. These occurred because the nanoparticles after formation, aggregates rapidly and formed clusters due to the magnetic nature of magnetite (Lim *et al*., 2013). After stabilising with

Copyright Reserved © NJMSE, 2020

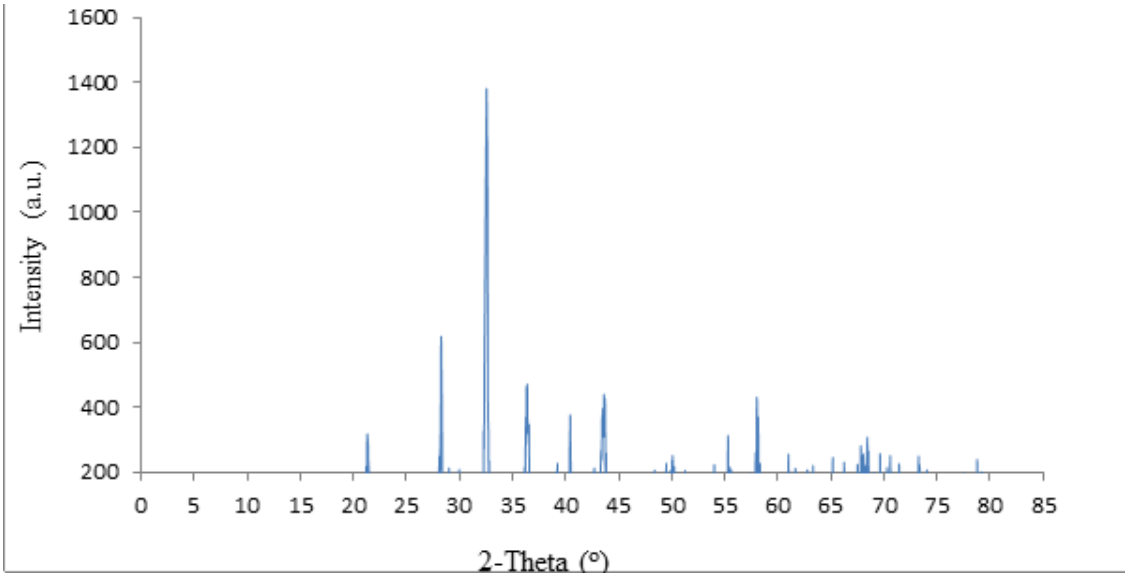


Figure 5: X-Ray Diffraction Pattern of Magnetite Nanoparticles

Table 9: XRD Parameters of Magnetite Nanoparticles

Diffraction Angle, 2θ, (°)	Peak Index (*h k l*)	Interplanar Spacing, d, (nm)	FWHM of the Intense Peak, β,(radians)	Crystallite Size, D, (nm)
21.34	1 1 1	0.42	0.0032	44.77
28.30	2 2 0	0.32	0.0022	66.46
32.59	-	0.27	0.0043	33.81
36.43	3 1 1	0.25	0.0047	31.28
40.48	-	0.22	0.0020	72.63
43.67	4 0 0	0.21	0.0069	21.63
50.15	-	0.18	0.0046	33.06
55.37	4 2 2	0.17	0.0009	183.24
58.08	5 1 1	0.16	0.0083	19.10
68.13	6 2 0	0.14	0.0116	14.41
			Particle Mean Crystallite Size = 52.04 nm	

nanoparticles at different magnifications are presented in Figure 6 (a-d). The micrograph in (a) indicates that there was aggregation of nanoparticles forming clusters which are cubical in nature. This is characteristic of magnetite nanoparticles. At higher magnifications, Figures 6(b – d), individual particles were observed to be spherical in shape and falls within a narrow range of size distribution. The particles have an average diameter of 9.5 nm.

The Energy Dispersive Spectrum from the high-resolution transmission electron microscopy studies (Figure 7) indicates the formation of iron oxides nanoparticles having very high intensity. Appearance of Fe at different energy keV is related to the formation of Fe_3O_4 nanoparticles. Aside the Fe peaks, the spectrum also indicated the presence of Al, Si, Mg, Cl, K, Ca and C having peaks of small intensities. The percentage of these elements is in very small amount judging from the intensity of their peaks. Their presence could be said to be related to the elements from the leave extracts used for the reduction of iron salts to magnetite. The presence of Cu is related to the material of the grid on which the sample was mounted during sample preparation and analysis.

It was observed that the particle size measurement obtained using the High transmission electron microscopy was lower than for the X-ray diffraction studies and the dynamic light scattering methods. This could be attributed to the fact that with HRTEM, the particle size, shape and distribution can easily be confirmed. The samples were however measured over a small selected area (Jarzębski *et al*., 2017). For measurement by Dynamic Light Scattering method,

Copyright Reserved © NJMSE, 2020

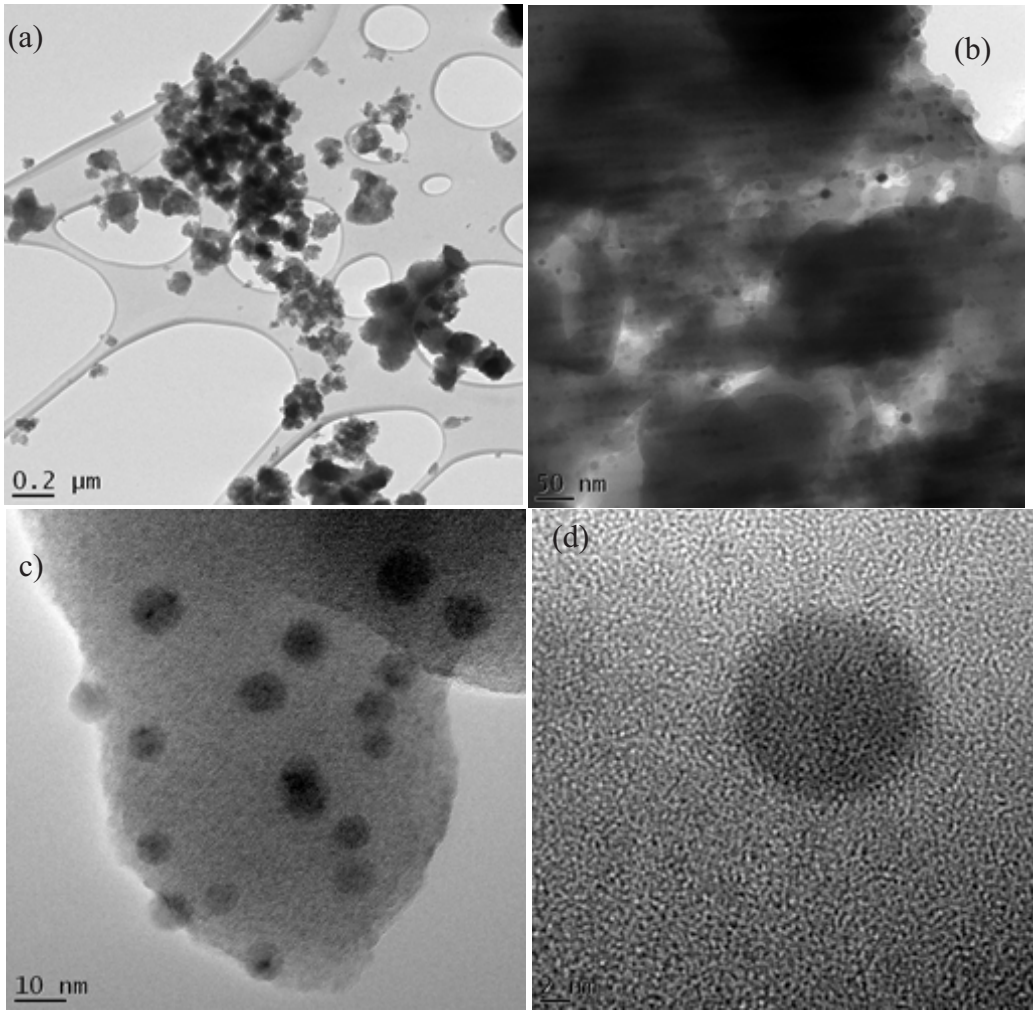


Figure 6: HRTEM of Magnetite Nanoparticles at different scales of magnification (a) 0.2 µm, (b) 50 nm, (c) 10 nm and (d) 2 nm

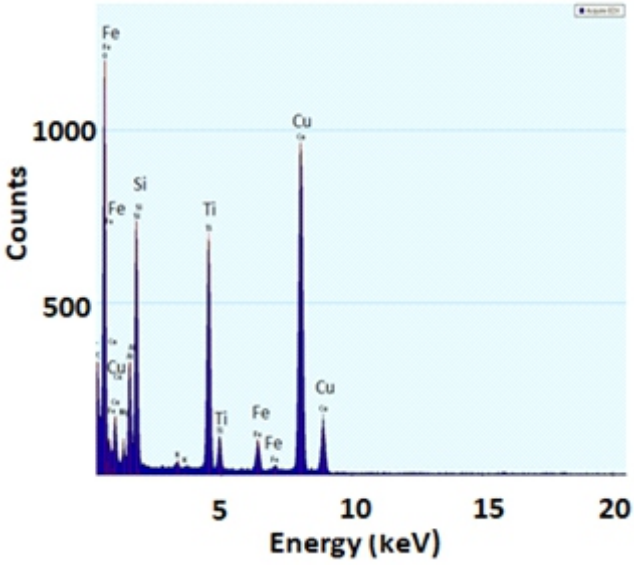


Figure 7: Energy Dispersive Spectrum of Magnetite Nanoparticles

surface coating of nanoparticles, rapid aggregation and subsequent formation of chain-like gelation with nanoparticles forming micron-size cluster is possible when sample are kept over a period of time (Lim *et al*., 2013).

3.6 Magnetic Characterisation of Nanoparticles

The result of the magnetic parameters of the synthesised magnetite nanoparticles is presented in the hysteresis loop in the Magnetisation-Magnetic Field Strength (M-H) curve presented in Figure 8. The magnetite nanoparticles sample has an average saturation magnetisation, Ms, of 3.54E-03 emu and average field strength applied of 4997.5. The area under the hysteresis loop (Oe*emu), for the sample was 4.44×10^{-2}. The magnetic permeability (emu/Oe) of the magnetite nanoparticles measured 8.39×10^{-7}. The magnetic permeability been less than 1.0 confirmed the diamagnetic behaviour of the sample.

Copyright Reserved © NJMSE, 2020

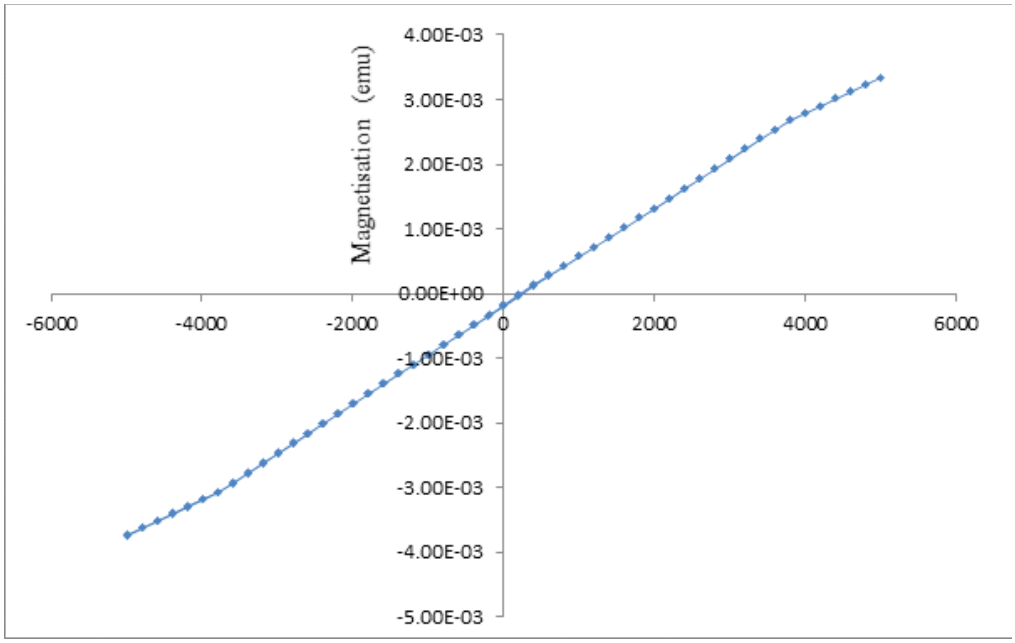


Figure 8: Magnetisation-Magnetic Field Strength (M-H) Hysteresis curve of Magnetite nanoparticles

4.0 CONCLUSION

In conclusion, the optimisation of green synthesis of magnetite nanoparticles was achieved using Fe^{3+} and Fe^{2+} precursors in ratio of 2:1 and extracts from mango leaves as reducing agent. Optimum synthesis parameters of volume of plant extract: volume of iron precursor of ratio of 15:1, temperature of 70°C, without stirring the reaction medium, was established for the production of magnetite nanoparticles. The magnetite nanoparticles produced by this condition have average hydrodynamic diameter particle size of 247.2 nm measured by Dynamic Light Scattering method. Dispersing the reaction medium with polyethylene glycol (PEG-2000), reduced the particle size further to 143.9 nm. High resolution transmission electron microscopy studies revealed that the magnetite nanoparticles are well distributed, spherical in shape, with a mean particle size of 9 nm. The hysteresis loop obtained by the vibrating sample magnetometer indicates the diamagnetic properties of the particles. The optimal synthesis parameters established proves as a viable route for green synthesis of magnetite nanoparticles for application in engineering, medicine, wastewater treatment and environmental remediation.

ACKNOWLEDGEMENT

The Africa Centre of Excellence for Mycotoxin and Food Safety, Federal University of Technology, Minna, NIGERIA is appreciated for the use of its facilities during the course of the research. The authors also wish to acknowledge Dr. Remy Bucher, iThemba Laboratories of South Africa for the use of the X-Ray Diffraction machine; Dr. Franscious Cummings, Physics Department, University of Western Cape, South Africa for the Use of High Resolution Transmission Electron Microscope and Mr. Collins Ofiwe of the NASENI Centre of Excellence in Nanotechnology and Advanced Materials for the use of Vibrating Samples Magnetometer.

REFERENCES

Al-Kalifawi, E. J. (2015). Green synthesis of magnetite iron oxide nanoparticles by using Al-Abbas's (A.S.) hund fruit (*Citrus medica*) var. Sarcodactylis Swingle extract and used in Al-'alqami river water treatment. *Molecules*, 18, 5954-5964. https://doi.org/10.3390/molecules18055954.ss

AOAC (1984). Official Methods of Analysis. Association of Official Analytical Chemists. 14th Ed., AOAC, Arlington.

Awwad, A. M. & Salem, N. M. (2012). A Green and Facile Approach for Synthesis of Magnetite Nanoparticles. *Nanoscience and Nanotechnology*, 2 (6), 208-213. https://doi.org/10.5923/j.nn.20120206.09

Bibi I., Nazara N., Atab, S., Sultan M., Ali, A., Abbasa, A., Jilani, K., Kamale S., Sarim, F. M., Khan, M. I., Jalal, F. & Iqbali, M. (2019). Green synthesis of iron oxide nanoparticles using pomegranate seeds extract and photocatalytic activity evaluation for the degradation of textile dye. *Journal of Materials Science and Technology*, 8 (6), 6115–6124. https://doi.org/10.1016/j.jmrt.2019.10.006

Cormode, D. P., Skajaa, T., Fayad, Z. A. & Mulder, W. J. M. (2009). Nanotechnology in Medical Imaging Probe Design and Applications. *Nanotechnology and Probe Design*, 992-1000. https://doi.org/10.1161/ATVBAHA.108.165506

Herlekar, M., Barve, S., & Kumar, R. (2014). Plant-Mediated Green Synthesis of Iron Nanoparticles.

Copyright Reserved © NJMSE, 2020

Journal of Nanoparticles, https://doi.org/10.1155/2014/140614

Jarzębski, M., Kościński M., & Białopiotrowicz, T. (2017). Determining the size of nanoparticles in the example of magnetic iron oxide core-shell systems. The 6th International Conference on Manufacturing Engineering and Process IOP Publishing IOP Conf. Series: Journal of Physics: Conf. Series 885 (2017) 012007. https://doi.org/10.1088/1742-6596/885/1/012007

Karkuzhali & Yogamoorthi, A. (2015). Biosynthesis of iron oxide nanoparticles using aqueous extracts of *Jathropha gosspifolia* as source of reducing agent. *International Journal of Nanoscience and Nanotechnology*, 6 (1), 47-55.

Kanagasubbulakshmi, S. & Kadirvelu, K. (2017). "Green Synthesis of Iron Oxide Nanoparticles using *Lagenaria Siceraria* and Evaluation of its Antimicrobial Activity". *Defence Life Science Journal*, 2 (4). https://doi.org/10.14429/ dlsj.2.12277

Kudr, J., Haddad, Y., Richtera, L., Heger, Z., Cernak, M., Adam, V. & Zitka, O. (2017). "Magnetic Nanoparticles: From Design and Synthesis to Real World Applications". *Nanomaterials*, 2017 (7), 243. https://doi.org/10.3390/nano7090243

Latha, N. & Gowri, M. (2014). "Bio-synthesis and characterisation of Fe_3O_4 nanoparticles using *Caricaya papaya* leaves extract". *International Journal of Science and Research (IJSR)*.11.

Lemes, M. A., Godinho, M. S., Rabelo, D., Martins, F. T., Mesquita, A., Neto, F. N., Araujo, O. A., Oliveira, A. E., (2014). "Estimating mean crystallite size of magnetite using multivariate calibration and powder x-ray diffraction analysis". *Acta Chim Slov.* 61(4), 778-85.

Lim, J., Yeap, S. P., Che, H. X & Low, S. C. (2013). "Characterization of magnetic nanoparticles by dynamic light scattering". *Nanoscale Research Letters*, 8 (381). http://www.nanoscalereslett.com/content/8/1/381

Mascolo, M. C., Pei Y., & Ring, T. A. (2013). "Room temperature co-precipitation synthesis of magnetite nanoparticles in a large ph window with different bases". *Materials*, 6, 5549-5567. https://doi.org/10.3390/ma612554

Mody, V. V., Cox, A., Shah, S., Singh, A., Bevins, W. & Parihar, H. (2014). "Magnetic nanoparticle drug delivery systems for targeting tumor". *Applied Nanoscience*, 4, 385–392. https://doi.org/10.1007/s13204-013-0216-y

Monshi, A., Foroughi, M. R. & Monshi, M. R. (2012). "Modified Scherrer Equation to Estimate More Accurately Nano-Crystallite Size Using XRD". *World Journal of Nano Science and Engineering*, 2012 (2), 154-160. https://doi.org/10.4236/ wjnse.2012.23020

Pattanayak, M. & Nayak, P. L. (2013). "Ecofriendly green synthesis of iron nanoparticles from various plants and spices extract". *International Journal of Plant, Animal and Environmental Sciences*. 3 (1), 68-78.

Pranita, L. & Preeti, J. (2015). Preparation and characterisation of zinc doped magnetite nanoparticles using green synthesis. *International Journal of Research in Chemistry and Environment,* 5 (4), 60-64.

Prasad, C., Gangadhara, S. & Venkateswarlu, P. (2016). Bio-inspired green synthesis of Fe_3O_4 magnetic nanoparticles using watermelon rinds and their catalytic activity. *Applied Nanoscience*, 6, 797–802. https://doi.org/10.1007/s13204-015-0485-8

Prasad, R., (2014). Synthesis of silver nanoparticles in photosynthetic plants. *Journal of Nanoparticles*, 2014, 1-9. https://doi.org/10.1155/2014/963961

Price, P. M., Mahmoud, W. E., Al-Ghamdi, A. A. & Bronstein, L. M. (2018). Magnetic Drug Delivery: Where the Field Is Going. *Frontier in Chemistry*, 6, 619. https://doi.org/10.3389/fchem.2018.00619

Priyadarshana, G., Kottegoda, N., Senaratne, A., Alwis, A. & Karunaratne V. (2015). Synthesis of Magnetite Nanoparticles by Top-Down Approach from a High Purity Ore. *Journal of Nanomaterials*. https://doi.org/10.1155/2015/317312

Ramesh, A. V., Devi, D. R., Botsa, S. M. & Basavaiah, K. (2018). "Facile green synthesis of Fe_3O_4 nanoparticles using aqueous leaf extract of *Zanthoxylum armatum* for efficient adsorption of methylene blue". *Journal of Asian Ceramic Societies*, 6 (2),145-155. https://doi.org/10.1080/21870764.2018.1459335

Rocha-Santos T. A. P. (2014). Sensors and biosensors based on magnetic nanoparticles. *Trends in Analytical Chemistry*,62,28–36. https://doi.org/10.1016/j.trac.2014.06.016

Ruíz-Baltazara Á. J., Reyes-Lópezb, S. Y., Mondragón-Sánchezc, M. L., Robles-Cortésc, A. I. & Pérezd R. (2018). Eco-friendly synthesis of Fe_3O_4 nanoparticles: Evaluation of their catalytic activity in methylene blue degradation by kinetic adsorption models activity in methylene blue degradation by kinetic adsorption models. *Results in Physics*, 12, 989 -995. https://doi.org/10.1016/j.rinp.2018.12.037

Saif, S., Tahir, A. & Chen, Y. (2016). Green synthesis of iron nanoparticles and their environmental applications and implications. *Nanomaterials*, 6 (11),1-26. https://doi.org/10.3390/nano6110209

Sathishkumar, G., Logeshwaran, V., Sarathbabu, S., Jha, P. K., Jeyaraj, M., Rajkuberan, C., Senthilkumar, N. & Sivaramakrishnan, S. (2018). Green synthesis of magnetic Fe_3O_4 nanoparticles using *Couroupita guianensis* Aubl. fruit extract for their antibacterial and cytotoxicity activities. *Artificial Cells, Nanomedicine, and Biotechnology*, 46 (3),589-598. https://doi.org/10.1080/21691401. 2017.1332635

Vangijzegem, T., Stanicki, D. & Laurent, S. (2019). Magnetic iron oxide nanoparticles for drug delivery: applications and characteristics. *Expert Opinion on Drug Delivery*, 16 (1),69-78. https://doi.org/10.1080/17425247.2019.1554647

Copyright Reserved © NJMSE, 2020

Veeramanikandan V., Madhu G. C., Pavithra V., Jaianand K & Balaji P. (2017). Green Synthesis, Characterization of Iron Oxide Nanoparticles using Leucas Aspera Leaf Extract and Evaluation of Antibacterial and Antioxidant Studies. *International Journal of Agriculture Innovations and Research*, 6 (2), 242-250.

Wallyn, J., Anton, N. & Vandamme, T. F. (2019). Synthesis, Principles, and Properties of Magnetite Nanoparticles for In Vivo Imaging Applications—A Review. *Pharmaceutics*, 11, 601. https://doi.org/10.3390/pharmaceutics11110601

Copyright Reserved © NJMSE, 2020